Variable multilayer reflection together with long-pass filtering pigment determines the wing coloration of papilionid butterflies of the *nireus* group

Tomasz M. Trzeciak,[1,*] Bodo D. Wilts,[2] Doekele G. Stavenga,[2] and Peter Vukusic[1]

[1]*School of Physics, Exeter University, Exeter EX4 4QL, UK*
[2]*Computational Physics, Zernike Institute for Advanced Materials, University of Groningen, NL-9747 AG, the Netherlands*
[*]*t.m.trzeciak@gmail.com*

Abstract: The dorsal wing surfaces of papilionid butterflies of the *nireus* group are marked by bands of brilliant blue-green-colored cover scales. The thin, cuticular lower lamina of the scales acts as a blue reflector. The thick upper lamina forms a dense two-dimensional cuticular lattice of air cavities with a pigment acting as a long-pass optical filter. Reflectance spectra of small scale areas oscillate, but for large scale areas and the intact wing they are smooth. Theoretical modeling shows that the oscillations vanish for a scale ensemble with varying layer thicknesses and cavity dimensions. The scales combine in a subtle way structural and pigmentary coloration for an optical effect.

OCIS codes: (160.1435) Biomaterials; (170.1420) Biology; (230.4170) Multilayers.

References and links

1. H. F. Nijhout, *The Development and Evolution of Butterfly Wing Patterns* (Smithsonian Institution Press, 1991).
2. H. Ghiradella, "Hairs, bristles, and scales," in *Microscopic Anatomy of Invertebrates*, M. Locke, ed. (Wiley-Liss, 1998), pp. 257–287.
3. N. I. Morehouse, P. Vukusic, and R. Rutowski, "Pterin pigment granules are responsible for both broadband light scattering and wavelength selective absorption in the wing scales of pierid butterflies," Proc. Biol. Sci. **274**(1608), 359–366 (2007).
4. B. Wijnen, H. L. Leertouwer, and D. G. Stavenga, "Colors and pterin pigmentation of pierid butterfly wings," J. Insect Physiol. **53**(12), 1206–1217 (2007).
5. S. M. Luke, P. Vukusic, and B. Hallam, "Measuring and modelling optical scattering and the colour quality of white pierid butterfly scales," Opt. Express **17**(17), 14729–14743 (2009).
6. M. Srinivasarao, "Nano-optics in the biological world: beetles, butterflies, birds, and moths," Chem. Rev. **99**(7), 1935–1962 (1999).
7. P. Vukusic and J. R. Sambles, "Photonic structures in biology," Nature **424**(6950), 852–855 (2003).
8. S. Kinoshita, *Structural Colors in the Realm of Nature* (World Scientific, 2008).
9. S. Kinoshita, S. Yoshioka, and J. Miyazaki, "Physics of structural colors," Rep. Prog. Phys. **71**(7), 076401 (2008).
10. L. P. Biró and J.-P. Vigneron, "Photonic nanoarchitectures in butterflies and beetles: valuable sources for bioinspiration," Laser Photonics Rev. **5**(1), 27–51 (2011).
11. L. P. Biró, K. Kértesz, Z. Vértesy, G. I. Márk, Z. Bálint, V. Lousse, and J.-P. Vigneron, "Living photonic crystals: butterfly scales - nanostructure and optical properties," Mater. Sci. Eng. C **27**(5-8), 941–946 (2007).
12. P. Vukusic, J. R. Sambles, C. R. Lawrence, and R. J. Wootton, "Quantified interference and diffraction in single *Morpho* butterfly scales," Proc. Biol. Sci. **266**(1427), 1403–1411 (1999).
13. S. Kinoshita, S. Yoshioka, and K. Kawagoe, "Mechanisms of structural colour in the Morpho butterfly: Cooperation of regularity and irregularity in an iridescent scale," Proc. Biol. Sci. **269**(1499), 1417–1421 (2002).
14. K. Kertész, Z. Bálint, Z. Vértesy, G. I. Márk, V. Lousse, J.-P. Vigneron, M. Rassart, and L. P. Biró, "Gleaming and dull surface textures from photonic-crystal-type nanostructures in the butterfly *Cyanophrys remus*," Phys. Rev. E Stat. Nonlin. Soft Matter Phys. **74**(2), 021922 (2006).
15. B. D. Wilts, H. L. Leertouwer, and D. G. Stavenga, "Imaging scatterometry and microspectrophotometry of lycaenid butterfly wing scales with perforated multilayers," J. R. Soc. Interface **6**(Suppl 2), S185–S192 (2009).

#162309 - $15.00 USD Received 31 Jan 2012; revised 23 Mar 2012; accepted 23 Mar 2012; published 2 Apr 2012

16. A. Argyros, S. Manos, M. C. Large, D. R. McKenzie, G. C. Cox, and D. M. Dwarte, "Electron tomography and computer visualisation of a three-dimensional 'photonic' crystal in a butterfly wing-scale," Micron **33**(5), 483–487 (2002).
17. K. Michielsen and D. G. Stavenga, "Gyroid cuticular structures in butterfly wing scales: biological photonic crystals," J. R. Soc. Interface **5**(18), 85–94 (2008).
18. K. Michielsen, H. De Raedt, and D. G. Stavenga, "Reflectivity of the gyroid biophotonic crystals in the ventral wing scales of the Green Hairstreak butterfly, *Callophrys rubi*," J. R. Soc. Interface **7**(46), 765–771 (2010).
19. B. D. Wilts, K. Michielsen, H. De Raedt, and D. G. Stavenga, "Iridescence and spectral filtering of the gyroid-type photonic crystals in *Parides sesostris* wing scales," Interface Focus, published online before print December 21, 2011, doi: *10.1098/rsfs.2011.0082* (2011).
20. V. Saranathan, C. O. Osuji, S. G. Mochrie, H. Noh, S. Narayanan, A. Sandy, E. R. Dufresne, and R. O. Prum, "Structure, function, and self-assembly of single network gyroid ($I4_132$) photonic crystals in butterfly wing scales," Proc. Natl. Acad. Sci. U.S.A. **107**(26), 11676–11681 (2010).
21. C. W. Mason, "Structural colors in insects. III," J. Phys. Chem. **31**(12), 1856–1872 (1927).
22. H. Ghiradella, "Structure and development of iridescent Lepidopteran scales - the Papilionidae as a showcase family," Ann. Entomol. Soc. Am. **78**, 252–264 (1985).
23. J. Huxley, "Coloration of *Papilio zalmoxis* and *P. antimachus*, and discovery of Tyndall blue in butterflies," Proc. R. Soc. Lond. B Biol. Sci. **193**(1113), 441–453 (1976).
24. R. O. Prum, T. Quinn, and R. H. Torres, "Anatomically diverse butterfly scales all produce structural colours by coherent scattering," J. Exp. Biol. **209**(4), 748–765 (2006).
25. P. Vukusic and I. Hooper, "Directionally controlled fluorescence emission in butterflies," Science **310**(5751), 1151 (2005).
26. D. G. Stavenga, H. L. Leertouwer, P. Pirih, and M. F. Wehling, "Imaging scatterometry of butterfly wing scales," Opt. Express **17**(1), 193–202 (2009).
27. P. Vukusic and D. G. Stavenga, "Physical methods for investigating structural colours in biological systems," J. R. Soc. Interface **6**(2 Suppl 2), S133–S148 (2009).
28. D. G. Stavenga, B. D. Wilts, H. L. Leertouwer, and T. Hariyama, "Polarized iridescence of the multilayered elytra of the Japanese jewel beetle, *Chrysochroa fulgidissima*," Philos. Trans. R. Soc. London Ser. B **366**(1565), 709–723 (2011).
29. S. J. Orfanidis, "Electromagnetic Waves and Antennas," *www.ece.rutgers.edu/~orfanidi/ewa/* (2010).
30. H. L. Leertouwer, B. D. Wilts, and D. G. Stavenga, "Refractive index and dispersion of butterfly chitin and bird keratin measured by polarizing interference microscopy," Opt. Express **19**(24), 24061–24066 (2011).
31. P. Vukusic, R. Sambles, C. Lawrence, and G. Wakely, "Sculpted-multilayer optical effects in two species of Papilio butterfly," Appl. Opt. **40**(7), 1116–1125 (2001).
32. B. D. Wilts, T. M. Trzeciak, P. Vukusic, and D. G. Stavenga, "Papiliochrome II pigment reduces the angle dependency of structural wing colouration in *nireus* group papilionids," J. Exp. Biol. **215**(5), 796–805 (2012).
33. D. J. Brink and M. E. Lee, "Confined blue iridescence by a diffracting microstructure: an optical investigation of the *Cynandra opis* butterfly," Appl. Opt. **38**(25), 5282–5289 (1999).
34. E. Nakamura, S. Yoshioka, and S. Kinoshita, "Structural color of rock dove's neck feather," J. Phys. Soc. Jpn. **77**(12), 124801 (2008).
35. D. G. Stavenga, J. Tinbergen, H. L. Leertouwer, and B. D. Wilts, "Kingfisher feathers - colouration by pigments, spongy nanostructures and thin films," J. Exp. Biol. **214**(23), 3960–3967 (2011).
36. H. Ghiradella, "Structure of iridescent Lepidopteran scales - variations on several themes," Ann. Entomol. Soc. Am. **77**, 637–645 (1984).
37. H. Ghiradella, "Light and color on the wing: structural colors in butterflies and moths," Appl. Opt. **30**(24), 3492–3500 (1991).
38. L. Poladian, S. Wickham, K. Lee, and M. C. Large, "Iridescence from photonic crystals and its suppression in butterfly scales," J. R. Soc. Interface **6**(2 Suppl 2), S233–S242 (2009).
39. M. Kolle, P. M. Salgard-Cunha, M. R. Scherer, F. Huang, P. Vukusic, S. Mahajan, J. J. Baumberg, and U. Steiner, "Mimicking the colourful wing scale structure of the *Papilio blumei* butterfly," Nat. Nanotechnol. **5**(7), 511–515 (2010).
40. M. Barbier, "The status of blue-green bile-pigments of butterflies, and their phototransformations," Experientia **37**(10), 1060–1062 (1981).
41. M. Choussy and M. Barbier, "Pigments biliaires des lépidoptères: identification de la phorcabiline I et de la sarpédobiline chez diverses espèces," Biochem. Syst. **1**(4), 199–201 (1973).
42. D. G. Stavenga, M. A. Giraldo, and H. L. Leertouwer, "Butterfly wing colors: glass scales of *Graphium sarpedon* cause polarized iridescence and enhance blue/green pigment coloration of the wing membrane," J. Exp. Biol. **213**(10), 1731–1739 (2010).

1. Introduction

The beautiful patterns displayed by butterflies are determined by the scattering properties of the scales that imbricate the wings [1]. Scattering arises when incident light interacts with the structural elements of the scales. Generally, these are composed of a more or less unstructured

#162309 - $15.00 USD Received 31 Jan 2012; revised 23 Mar 2012; accepted 23 Mar 2012; published 2 Apr 2012

lower lamina and a highly structured upper lamina. The upper lamina is marked by longitudinal ridges that are connected by crossribs. Pillar-like cuticular structures, trabeculae, often connect both laminae [2]. The scales have a pigmentary coloration when they contain pigments that absorb in a specific wavelength range. This is the dominant coloration method of most butterfly species, especially in many nymphalids and pierids [1,3–5]. However, a structural coloration arises when the scale structures have periodicities in the nanometer range [6–10]. The best studied example of structural coloration is that of *Morpho* butterflies, which have scale ridges folded into multilayers, causing a striking, metallic-blue color [11–13]. Many lycaenids (Polyommatinae and Theclinae) exhibit metallic blue and green structural colours due to multilayers in the wing scale interior [11,14,15], while other lycaenids (e.g. *Callophrys rubi*) and also papilionids (e.g. *Parides sesostris*) create diffuse green colorations with gyroid scale structures [7,16–20].

The forewings and hindwings of the four papilionid species investigated in this paper, *Papilio bromius*, *P. epiphorbas*, *P. nireus*, and *P. oribazus*, belonging to the *nireus* group, are dorsally marked by brilliant blue-green bands surrounded by black margins (note: the nomenclature of the species is not unambiguous; here we follow WorldFieldGuide.com: http://www.worldfieldguide.com/wfg-species-detail.php?taxno=8552). The striking coloration has been studied by several investigators, who put forward a variety of interpretations. Firstly, Mason [21] compared the coloration and scale structure of *Papilio nireus* and *P. zalmoxis* and remarked that their scales are essentially similar. He stated that there is a 'mesh structure on the upper surface of the scales, which gives them a matte lustre. The seat of the iridescence is beneath this layer, and is very brilliant from the underside of the scale.' (ref [21], p. 335, 336). Huxley, in his detailed study of the blue scales of *P. zalmoxis*, found that the upper lamina of the colored cover scales contained a most elaborate formation of crossribs creating a network of channels. He also noted that the cover scales of *P. zalmoxis* exhibited a distinct fluorescence and that the cover scales of '*P. bromius* appear identical in structure, as judged from scanning electron micrographs (SEMs) of the upper surface, and also contain a blue-fluorescing pigment. The blues of the species-group to which *bromius* belongs all look rather similar and are very likely generated in the same way'. Ghiradella [22] similarly reported that 'in the cover scales of *Papilio epiphorbas*, *P. nireus*, *P. oribazus*, and *P. zalmoxis*, the network is refined into a series of regular channels'. Huxley [23], who called the channels alveoli, hypothesized that they caused the bluish scale color by Tyndall scattering. This view was critically challenged by Prum and associates [24], who argued that the closely packed cavities cannot be considered as independent scatterers, and they therefore concluded that the scales derive their color from coherent scattering in the regular array of cavities in the upper lamina. Vukusic and Hooper [25] on the other hand proposed that not only is the fluorescence emission of the wing scales influenced by the cylindrical air cavities in the scales' upper lamina, but that it is also directionally controlled by the presence of a three-layer distributed Bragg reflector (DBR) that forms the scales' bottom lamina and which is tuned in its reflectance with the fluorescence emission band.

We have revisited the complex coloring system of the *nireus* group of butterflies by applying a variety of optical methods, among others (micro)spectrophotometry and imaging scatterometry, to unravel the spectral and spatial reflection properties of the papilionid scales. In addition, we have performed scanning electron microscopy to determine the scale parameters, and we have applied computational modeling of the scale structures to interpret the measured reflectance spectra quantitatively.

#162309 - $15.00 USD Received 31 Jan 2012; revised 23 Mar 2012; accepted 23 Mar 2012; published 2 Apr 2012

2. Materials and methods

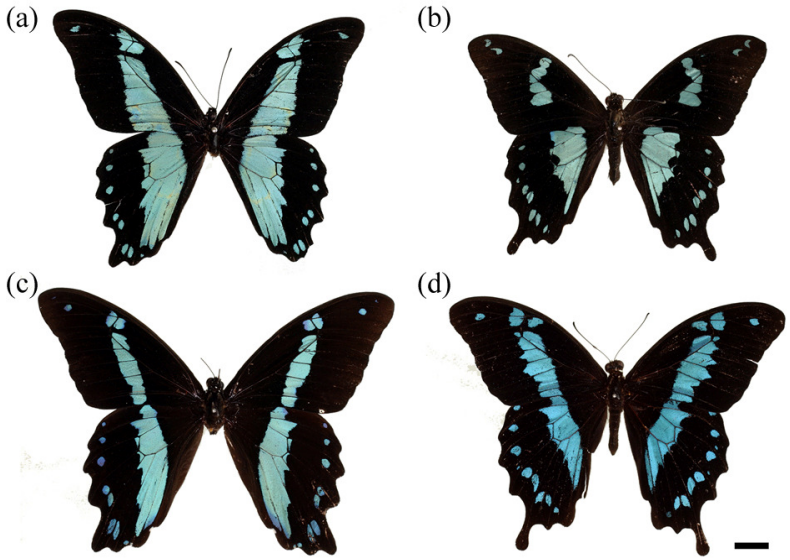

Fig. 1. Photographs of the dorsal wings of the four investigated papilionid butterflies of the *nireus* group: (a) *P. bromius*, (b) *P. epiphorbas*, (c) *P. nireus* and (d) *P. oribazus* (scale bar: 1 cm).

2.1 Animals

The optical properties of the wings of four closely related papilionid species were investigated: *Papilio bromius*, *P. epiphorbas*, *P. nireus*, *P. oribazus*. Specimens were obtained from World Wide Butterflies (Dorset, UK).

2.2 Photography

Specimens were photographed using a Canon EOS 30D camera equipped with an F70 macro objective.

2.3 Imaging scatterometry

The far-field angular distribution of the light scattered from single scales and wing patches, glued to the end of pulled micropipettes, was visualized with an imaging scatterometer (ISM; Refs [26,27].). The scatterometer is built around an ellipsoidal mirror, which collects light from a full hemisphere around its first focal point where the sample is positioned. A small piece of magnesium oxide served as a white diffusive reference object. Images were acquired with an Olympus DP-70 camera and were subsequently corrected for geometrical distortions using a MATLAB-routine. Spectra of certain points from the scatterogram were measured with a CCD detector array spectrometer (AvaSpec-2048-2; Avantes, Eerbeek, the Netherlands), which was connected to the beam path via an additional half-mirror and a bifurcated light-guide [28].

2.4 Spectrophotometry

Reflectance spectra of intact wings were measured with an integrating sphere (Avantes Avasphere-50-Refl) connected to the AvaSpec-2048-2 spectrometer. The light source was a xenon or a Deuterium-Halogen (Avantes D(H)-S) lamp, and the angle of illumination was about 8° with respect to the normal to the wing surface. Reflectance spectra of small scale patches (cross-section varied between ca. 5-40 μm^2) were measured on single scales in air with a microspectrophotometer utilizing the spectrometer. Transmittance spectra of single

#162309 - $15.00 USD Received 31 Jan 2012; revised 23 Mar 2012; accepted 23 Mar 2012; published 2 Apr 2012

wing scales immersed in a fluid with refractive index 1.56 were measured also with the microspectrophotometer. A white diffusing reference tile (Avantes WS-2) served as reference.

2.5 Anatomy

The structure of the wing scales was investigated, after sputtering with palladium, by SEM using a Philips XL30-ESEM and a FEI Novalab 600 Dual beam SEM. The upper lamina of the cover scales of the investigated papilionids was found to consist of cylindrical cavities. The filling fraction of the material creating the holes was estimated by thresholding the greyscale SEM images into a black-and-white mask that discriminated the scale material from the cylindrical voids and then calculating the fraction of white pixels. In addition to the SEM, transmission electron microscopy (TEM) sections were observed with a JEOL 110S TEM instrument (see ref [12].).

2.6 Modeling

Multilayer modeling was performed using MATLAB-routines for recursive Fresnel equations adapted from Orfanidis [29].

3. Results

3.1 Reflectance spectra of the colored wing areas are due to the cover scales

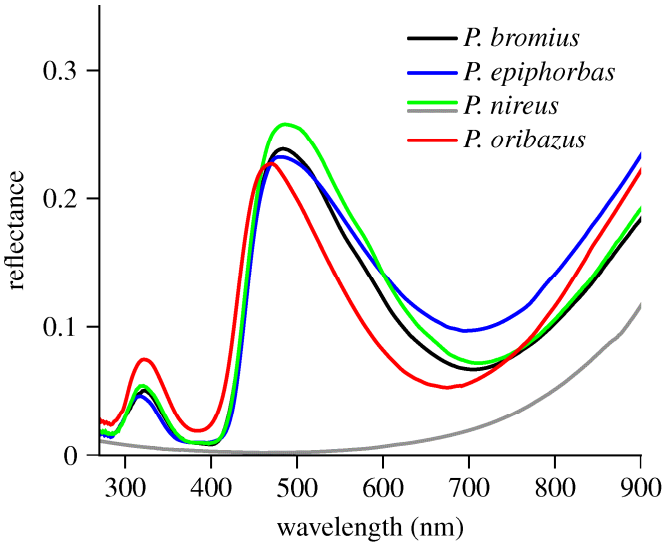

Fig. 2. Reflectance spectra of the colored bands in the wings of the four butterfly species of Fig. 1 (colored curves), together with a reflectance spectrum of the black marginal area of *P. nireus* (gray curve), measured at near normal illumination (~8°) with an integrating sphere.

The upperside of the wings of the four investigated papilionid butterfly species are marked by similar blue-green colored bands (Fig. 1). The bands slightly differ in color hue and pattern, locally throughout each wing and also among the species.

To characterize the colored bands we have measured reflectance spectra from small wing areas with an integrating sphere [27]. The reflectance spectra of the four species appear to be very similar, showing a main, somewhat asymmetric band with a maximum at about 500 nm, with a minor side band near 300 nm (Fig. 2). There is also a steady rise of the reflectance above 800 nm. The main reflectance band of *P. oribazus* is marginally blue-shifted compared to that of the other species (Fig. 1(d)).

#162309 - $15.00 USD Received 31 Jan 2012; revised 23 Mar 2012; accepted 23 Mar 2012; published 2 Apr 2012

Microscopic observation immediately showed that the primary colored elements of the wings are the cover scales. The underlying ground scales are dark brown or black (Fig. 3), like all scales in the darkly colored wing margins.

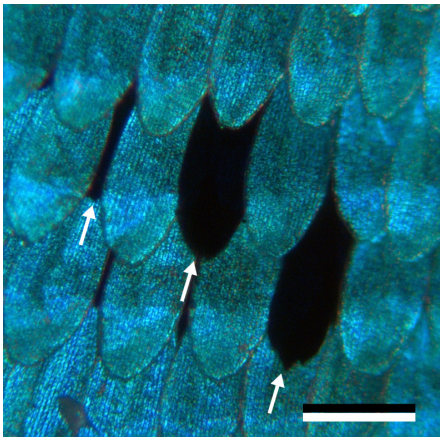

Fig. 3. Epi-illumination light microscopic image of a colored wing area of *P. oribazus*. The cover scales have a distinct blue color. The ground scales have a dark brown color (arrows; scale bar: 100 µm).

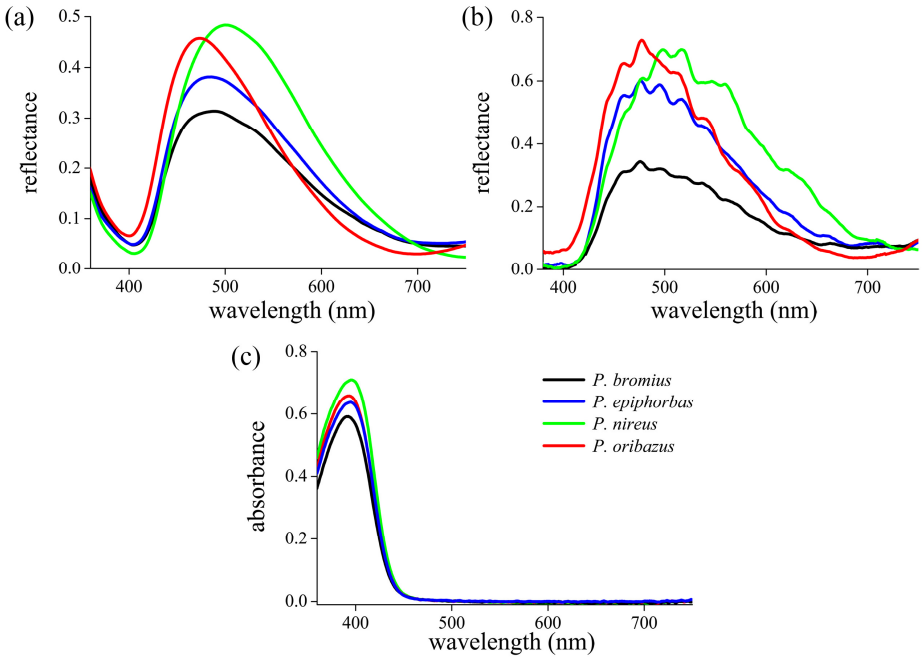

Fig. 4. Reflectance and absorbance spectra of single, isolated wing scales of the four investigated papilionids measured with a microspectrophotometer (MSP). (a) Reflectance spectra measured at the upperside of single scales from an area 30x30 µm^2. (b) Reflectance spectra measured from an area 4x4 µm^2. (c) Absorbance spectra calculated from transmittance spectra measured from single scales immersed in refractive index matching fluid.

Not surprisingly, reflectance spectra measured from individual, isolated cover scales with a microspectrophotometer (Fig. 4) closely resembled the spectra measured from the intact wing (Fig. 2). The reflectance amplitude slightly varied across the scale surface. When the measurement area spanned almost the whole scale's width, the spectra were smooth (Fig.

#162309 - $15.00 USD Received 31 Jan 2012; revised 23 Mar 2012; accepted 23 Mar 2012; published 2 Apr 2012

4(a)). However, when the measurement area was made small (of the order of a few micrometer in diameter), the spectra exhibited an oscillatory fine structure (Fig. 4(b)).

3.2 Pigmentation of the scales

Observing the scales with an epi-illumination microscope and applying ultraviolet (or blue) illumination revealed that the colored scales exhibit a distinct blue-green fluorescence. The scales hence must contain a short-wavelength absorbing pigment, which will affect the reflectance spectrum. To determine the absorbance spectrum of the pigment, we measured the transmittance of isolated scales while effectively eliminating the light loss due to scattering by immersing the scales in a fluid with refractive index 1.56, matching the refractive index of the scale material [12,30]. The cover scales of the four papilionids all showed very similar absorbance spectra restricted to the (ultra)violet wavelength range and with a maximal absorbance of ~0.5-0.7 at the peak wavelength of ~390 nm (Fig. 4(c)). The absorbance peak coincides with the minimum in the reflectance spectra.

3.3 Spatial distribution of the scale reflections

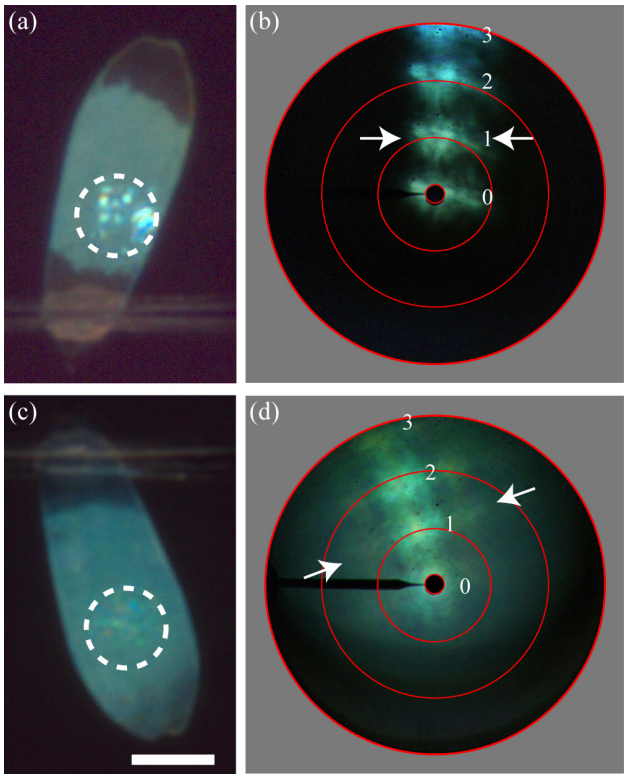

Fig. 5. Near-field (a, c) and superimposed far-field scatterograms (b, d) for the underside (a, b) and upperside (c, d) of a single scale of *P. epiphorbas*. A scale area with ~40 µm diameter (dashed circle) was illuminated with a narrow-aperture (5°) white beam. The scale was rotated in three steps of 15° (from normal (0°), to 15°, 30°, and 45°; numbered 0, 1, 2, 3, respectively), causing a change of 30° in the direction of the reflected light beam (from normal, 0°, to 30°, 60°, and 90°); the arrows indicate the first 15° step. The red circles indicate angular directions with respect to the axis of 5°, 30°, 60°, and 90° (scale bar for (a) and (c): 50 µm).

To investigate the spatial reflection characteristics of the cover scales, we isolated single scales and then glued the individual scales at the tip of a glass pipette. We positioned the scale at the first focal point of the imaging scatterometer and illuminated a small area of either the scale underside or upperside with a narrow-aperture, focused light beam (circles in Fig. 5(a),

#162309 - $15.00 USD Received 31 Jan 2012; revised 23 Mar 2012; accepted 23 Mar 2012; published 2 Apr 2012

5(c)), and monitored the spatial distribution of the far-field scattered light (Fig. 5(b), 5(d)). As can be seen from the spotty appearance of the near-field reflection pattern, the scale underside was clearly not perfectly flat (Fig. 5(a)). The near-field photographs are, like the applied illumination, limited by the 5° aperture of the central hole in the ellipsoidal mirror of the scatterometer. The far-field reflection pattern appeared nevertheless to be highly directional, with a spread of no more than a few degrees. The deviations from flatness are therefore minor. Rotation of the scale in steps of 15° resulted in a shift of the reflection pattern in steps of 30°, which demonstrated that the scale underside reflected specularly. With increasing angle of incidence, the pattern's color became more bluish. Such an iridescence phenomenon is a well-known property of reflecting multilayers [8,9].

Illumination of the upperside of the scale also yielded a slightly spotted pattern in the near-field, although more diffuse than that of the underside (Fig. 5(c)). The pattern's center closely resembles the reflection spots obtained from the scale's underside. Rotation of the scale in steps of 15° again resulted in displacements of the reflection pattern in steps of 30° (Fig. 5(d)). The iridescence, that is the color change of the reflection pattern with increasing angle of incidence, was less prominent than that of the underside, however (Fig. 5(b)). Furthermore, the reflection pattern of the upperside, although quite directional, was slightly more diffuse than that of the underside.

3.4 Cover scale anatomy and refractive indices

Knowledge of the scales' nanostructure is a requirement for a quantitative interpretation of the measured spectra as well as of their spatial reflection characteristics. For this reason we studied the anatomy of single scales using scanning electron microscopy (SEM) and transmission electron microscopy (TEM). Figure 6(a) presents a SEM-image from a cover scale of *P. nireus* cut with a razor blade, showing a thick upper lamina and a thin lower lamina, with trabeculae in between. Longitudinal ridges extend above the upper lamina, which appears to contain a matrix of cuticle with cylindrical air cavities arranged in a disordered lattice (Figs. 6(a), 6(b) and 7(a)). The hole-lattice layer has a thickness of approximately 1 μm and is separated by an about 1.5 μm thick space containing the sparsely distributed thin pillars (the trabeculae) above the lower lamina (Fig. 6(a), 6(b)). The lower lamina is relatively thin (ca. 200 nm) and comprised of three distinctive layers visible in TEM (Fig. 6(b)). The thicknesses of these three layers are approximately 75 nm, 50 nm and 75 nm [25]. The outer layers of the lower lamina showed a much higher contrast, indicating the presence of pigment in the cuticle [31]. The diagram of Fig. 6(c) shows an idealized and simplified version of the scale structure.

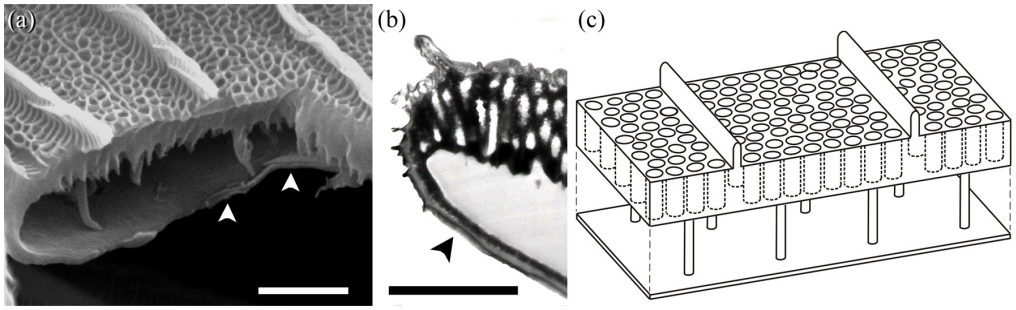

Fig. 6. Anatomy of the cover scales of the papilionids of Fig. 1. (a) A SEM image of a cut cover scale of *P. bromius* shows an upper lamina with thickness of approx. 1 μm, with ridges. The upper lamina has cylindrical cavities and rests on small pillars controlling the distance to the cuticle-air-cuticle triple layer (white arrows; scale bar: 2 μm). (b) TEM image of *P. nireus* showing the internal scale structure of the upper lamina of the scale and the lower lamina, which consists of three layers; the two outer layers are pigmented (black arrow; scale bar: 1 μm). (c) Diagram of the cover scale of the four investigated papilionid species.

#162309 - $15.00 USD Received 31 Jan 2012; revised 23 Mar 2012; accepted 23 Mar 2012; published 2 Apr 2012

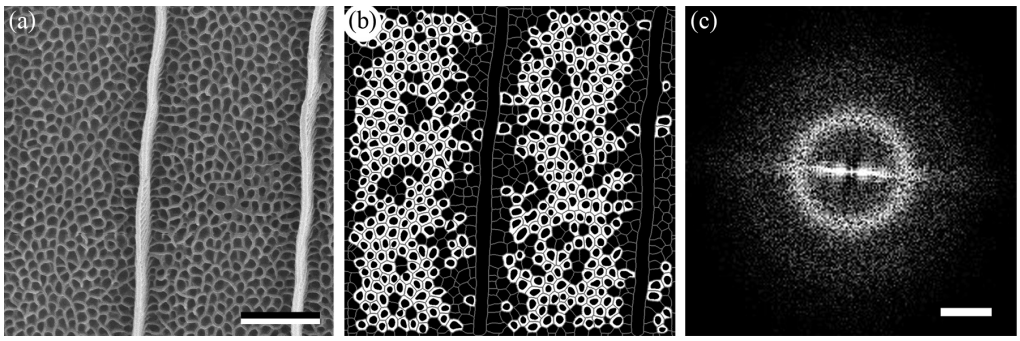

Fig. 7. Arrangement of the cavities in the upper lamina of the cover scales. (a) Top-view of the scale structure in *P. oribazus* (SEM image). (b) Result of the image analysis routine after segmentation of (a); only the image portion spanned by the white areas and the holes they contain was used for further data analysis. (c) Fast Fourier Transform (FFT) of (a). The ring-like structure indicates the order of the air holes (scale bars, in (a) and (b): 2 μm; in (c): 0.02 nm^{-1}).

For close to normal light incidence, the upper lamina can be treated to a first approximation as a uniform layer. Together with the three layers of the lower lamina and the air space in between the upper and lower lamina, the scale thus becomes effectively a 5-layer system with layer thicknesses approximately 1000, 1500, 75, 50 and 75 nm, respectively. For quantitative modeling of the multilayer's reflectance the refractive indices of the layers have to be known. The refractive index of the air space between the laminae, with thickness 1500 nm, is close to 1.0, because of the minor volume occupied by the trabeculae and other filaments. The refractive index of the other, dark stained layers is complex in the wavelength range < 450 nm, i.e., where the pigment absorption is substantial and leads to fluorescence emission. The contribution of the fluorescence to the overall appearance is, however, negligible [32]. The real part of the refractive index of the scale medium, chitin, can be assumed to be 1.56 [12,30]. However, this value is only appropriate for the cuticle layers of the lower lamina. Because of the cylindrical air-filled cavities traversing the upper lamina, the effective refractive index of the upper lamina will be reduced in proportion to the filling fraction of the cuticle. The fraction of the upper lamina taken up by the cuticle was estimated by analyzing top-view SEM images (Fig. 7(a)). The images were first segmented into regions containing individual cavities with subsequent thresholding of each region to discriminate between the air cavities and the cuticle. However, thresholding of the whole image with a fixed grey level value lead to poor results due to variation of the image background intensity and presence of the scale ridges. For this reason a multi-step image processing procedure was applied. The processing started with pre-filtering to remove high frequency noise, followed by segmentation with the watershed transform and auto-thresholding of each segmented region. To limit bias coming from image processing artifacts only regions with the Euler number equal to zero were retained in the analyses, i.e., we considered only the regions containing just one hole. The filling fraction was obtained by calculating the fraction of white pixels in the retained regions of the thresholded image (Fig. 7(b)). The values calculated for the four papilionid species appeared to be very similar (Table 1). The mean, area-equivalent diameter of the segmented regions was ~320 nm and the filling fraction of the cuticle ~0.64.

Table 1. Mean values and standard deviations for distributions of area equivalent diameter and cuticle filling fraction.

species	diameter (nm)	filling fraction
P. bromius	321 ± 26	0.644 ± 0.026
P. epiphorbas	328 ± 29	0.657 ± 0.034
P. nireus	332 ± 34	0.636 ± 0.030
P. oribazus	315 ± 28	0.635 ± 0.030

#162309 - $15.00 USD Received 31 Jan 2012; revised 23 Mar 2012; accepted 23 Mar 2012; published 2 Apr 2012

Figure 7(a) shows that the cavities in the upper lamina form a rather irregular pattern. To determine the order of the cylindrical air-hole structure, we applied a Fast Fourier Transform (FFT) to Fig. 7(a). This yielded a uniform ring-like pattern together with a patterned, about horizontal line (Fig. 7(c)). The ring indicates a close-range order, which is angularly isotropic. The radius of the ring is 0.022 nm^{-1}, which translates to an ensemble periodicity of the cavities of 285 nm. The horizontal line pattern in Fig. 7(c) arises due to the vertical scale ridges of Fig. 7(a).

With the cuticle filling fraction value 0.64 and the (real part of the) refractive index 1.56, the (real part of the) effective refractive index of the upper lamina becomes $1.56 \times 0.64 + 1 \times 0.36 = 1.36$. If the fluorescent pigment is uniformly distributed in the pigmented (dark stained) cuticular media of the upper and lower lamina, the effective thickness of the scale's absorbing media in the transmittance measurements was $d = (1000 \times 0.64) + 75 + 75 = 790$ nm. The peak absorbance was about $A = 0.60$ at wavelength $\lambda = 390$ nm, or the absorbance coefficient there is $\kappa = \ln(10)\, A/d = 0.0035$ nm^{-1}. The imaginary part of the refractive index at 390 nm then is $\mathrm{Im}(n) = \kappa\lambda/(4\pi) = 0.11$. Consequently, the complex refractive index of the two 75 nm thick layers of the lower lamina is 1.56-0.11i at 390 nm, and the peak effective refractive index of the 1000 nm thick upper lamina is 1.36-0.07i. These values were used in the following calculations of the reflectance spectrum of the 5-layer system of the scale, using classical multilayer theory.

3.5 Modeling the scale reflectance spectra

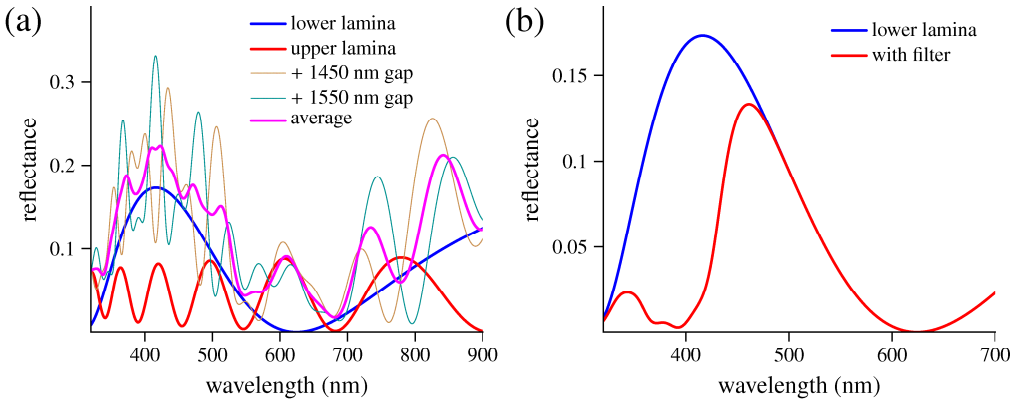

Fig. 8. Reflectance spectra calculated for various multilayers for normal light incidence. (a) Reflectance spectra of the lower lamina, with thickness 200 nm and refractive index 1.56 (blue curve), of the isolated upper lamina, with thickness 1000 nm and effective refractive index 1.36 (red curve), and of the 3-layer system, consisting of the lower and upper lamina with either a 1450 or a 1550 nm air gap in between. The magenta curve is the average of the latter two, highly oscillating spectra. (b) The reflectance spectrum of the lower lamina of (a) together with the spectrum obtained by filtering this spectrum by the pigmented upper lamina which has the absorbance spectrum of Fig. 4(c) (compare the resulting red curve with Fig. 4(a)).

As an example, Fig. 8(a) shows the reflectance spectra of the lower lamina and the upper lamina considered separately. Because the pigment absorbs only in the short-wavelength range, we first neglected the pigment absorbance, i.e., we assumed the refractive indices to have the same real value at all wavelengths, thus reducing the 5-layer system into a 3-layer system. The lower lamina then has a very broad-band reflectance spectrum peaking in the blue wavelength range, at ~400 nm (Fig. 8(a)). The reflectance spectrum of the upper lamina is highly oscillatory with a periodicity decreasing with increasing wavelength (Fig. 8(a)). Figure 8(a) also shows reflectance spectra of the combined system of lower and upper lamina separated by an air layer of 1450 or 1550 nm. The spectra show the features of both subsystems; a main broad band, modulated with high periodicity (Fig. 8(a)). The upper lamina

#162309 - $15.00 USD Received 31 Jan 2012; revised 23 Mar 2012; accepted 23 Mar 2012; published 2 Apr 2012

strongly modulates the reflectance spectrum of the lower lamina but otherwise seems to contribute relatively little to the overall magnitude of the reflectance, because the average of the two reflectance spectra obtained with air gap thicknesses 1450 and 1550 nm approximates the spectrum calculated for the isolated lower lamina. The spectra deviate somewhat at the longer wavelengths, where the reflectance of the lower lamina is minor.

The experimental reflectance spectra measured from large scale areas were smooth, but those measured from smaller areas featured modulations (Fig. 4(a), 4(b)). The wavelengths of the local maxima and minima slightly varied among the different locations (not shown), indicating that the thicknesses of the scale layers vary across the scale. Due to this thickness variation, the modulations in the reflectance spectra of larger areas vanish. The upper lamina with its violet-absorbing pigment (Fig. 4(c)) can then be treated as a simple long-pass filter in front of the reflective lower lamina. Taking a value 0.07 at 390 nm for the imaginary refractive index of the upper lamina, the reflectance spectrum of the lower lamina (Fig. 8(a), 8(b), blue curves) is strongly long-wavelength shifted to a spectrum peaking at ~470 nm (Fig. 8(b), red curve), very similar to the reflectance spectra measured from intact scales (Fig. 4(a), 4(b)).

3.6 Effects of locally scaled variations

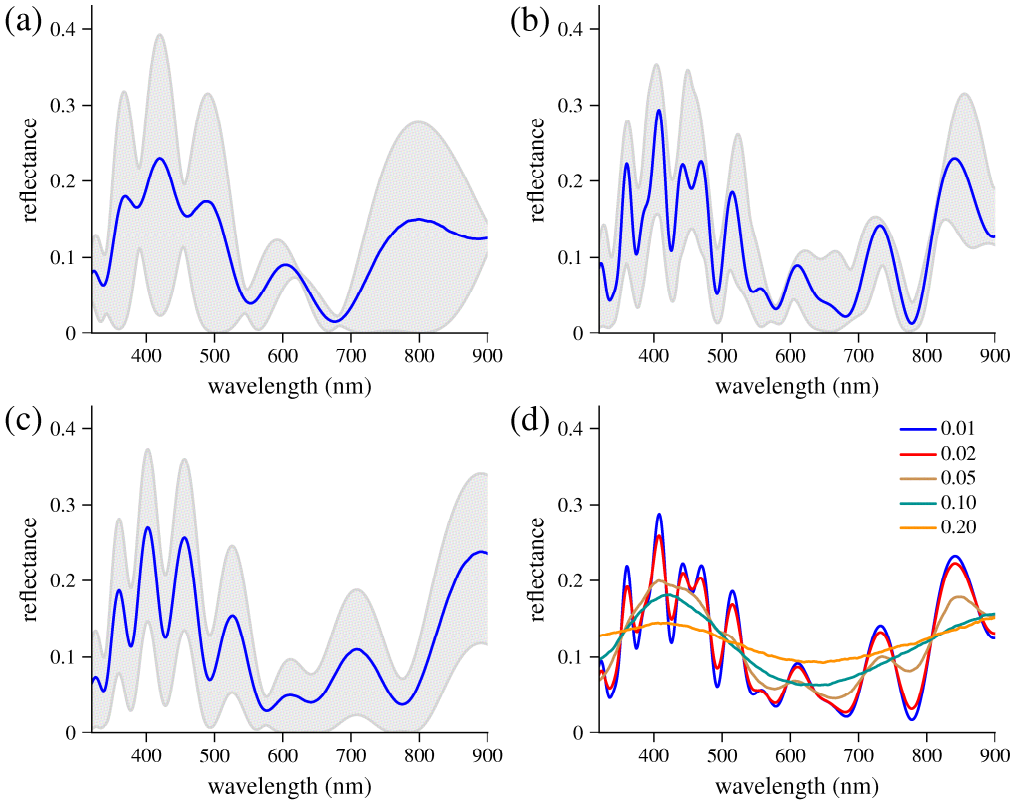

Fig. 9. Reflectance spectra when the thicknesses of the three layers of the cover scales vary stochastically. Averaged reflectance spectra (blue curves) resulting from a 10% variation in the distance between the lower and upper lamina (a), the filling fraction of the upper lamina (b), and the thickness of the upper lamina (c). (d) Averaged reflectance spectra resulting from simultaneous variation of all thicknesses in the 3-layer system with different amounts of added noise. An increase in noise leads to a progressive smoothing of the spectra.

We have further investigated the extent to which the modulations in the reflectance spectra will be smoothed due to variations in the scale parameters. We therefore have calculated the

#162309 - $15.00 USD Received 31 Jan 2012; revised 23 Mar 2012; accepted 23 Mar 2012; published 2 Apr 2012

averaged reflectance spectrum for an unpigmented 3-layer system, while varying the thicknesses of the individual layers stochastically. The amount of introduced randomness was controlled by specifying the standard deviation of the layers' thicknesses as a percentage of their mean value. A gamma distribution was used for generating random samples to ensure non-negative values. Reflectance spectra were obtained as an average from a few thousand random structures generated per each wavelength of the spectrum. Thus obtained spectra were then smoothed for presentation, but just enough to remove the noise inherent in stochastic simulation and without affecting them otherwise.

Figure 9(a) shows the average reflectance spectrum resulting from a varying air gap thickness between the upper and lower lamina, and the minimum-maximum envelope of attainable reflectance values is shown as the shaded region. It is apparent that the modulations cannot be fully removed through variation of this parameter alone. Figure 9(b) shows the average reflectance spectrum calculated for a varying filling fraction of the upper lamina. The distribution of the filling fraction could be obtained quite accurately from the image analysis of SEM micrographs and was approximated by a beta distribution for the purpose of practical computations in order to restrict the sampled values of the filling fraction to the range between 0 and 1. There is only a very minor influence of this parameter and the averaged spectrum is in fact nearly the same as the one obtained for the mean value of the filling fraction (Fig. 9(b)). Figure 9(b) also shows an envelope of minimum and maximum reflectance values attainable by varying the filling fraction. It is again clear that changing this parameter alone is not sufficient to remove the modulations from the spectrum. Figure 9(c) shows the average reflectance spectrum of the spectra calculated by varying only the thickness of the upper lamina, which leads to the same conclusion. Finally, the combined effect of varying together the thicknesses of all layers comprising the scale structure is shown in Fig. 9(d) for several different levels of the added noise. With increasing level of randomization, the reflectance spectrum becomes progressively smoother up to about 5-10% variation from the mean values of these parameters. Beyond this point the spectrum starts to flatten and becomes increasingly featureless (whitish) for highly randomized structures. Thus, this 5-10% randomization is optimal with respect of removing the effect of modulation but without affecting the overall color.

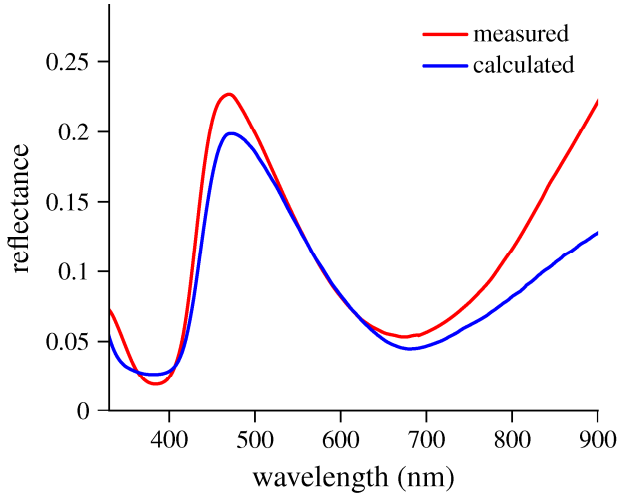

Fig. 10. Reflectance spectrum of *P. oribazus* measured with an integrating sphere and the spectrum calculated for a 3-layer 1000/1500/220 nm system with 10% variation in both the thickness of the (absorbing) upper lamina and its distance from the lower lamina.

With a suitable choice of thickness parameters for the upper and lower scale lamina and the level of their randomization it is in fact possible to approximate the experimentally

#162309 - $15.00 USD Received 31 Jan 2012; revised 23 Mar 2012; accepted 23 Mar 2012; published 2 Apr 2012

measured spectra fairly closely, not only in shape but also in magnitude. An example is shown in Fig. 10 for the total reflectance of the colored patches on wings of *P. oribazus* from Fig. 2. The modeled spectrum was calculated for the 1000/1500/220 nm 3-layer system, with 10% randomization of the upper lamina thickness and its distance from the lower lamina and including the effect of absorption in the top layer. Absorption in the lower lamina is essentially negligible and is thus neglected from the analysis. For these parameters the modeled spectrum is in fairly good agreement with the measured spectrum, except for the infrared region, where an increasing discrepancy is observed at longer wavelengths. This discrepancy presumably originates from the increased contribution to the total reflectance signal coming from the black ground scales lying beneath the colored cover scales (cf. reflectance of black and colored patches from *P. nireus* in Fig. 2).

4. Discussion

The wings of papilionid butterfly species of the *nireus* group are colored due to special structured cover scales. The scales consist of a lower and an upper lamina, which together reflect mainly the blue-green component of incident light in an approximately mirror-like fashion. Comparing the directional reflection of the scale's underside and upperside shows that the upper lamina, which consists of a mesh of air cavities, causes a slight angular spreading of the reflected light (Fig. 5). The isolated lower lamina has a broad-band reflectance spectrum, covering the ultraviolet to green wavelength range (Fig. 8). In the intact scale, the upper lamina in principle causes severe modulations of the reflectance spectrum, but these oscillations are effectively smoothed out due to inhomogeneities in the thickness of the laminae, in the filling fraction of the upper lamina, and in the distance between upper and lower lamina (Fig. 9). The scale's broad-band reflectance spectrum is curtailed to the blue-green due to the presence of a selectively (ultra)violet-absorbing pigment (Fig. 4(c)).

Our findings confirm the early observations of Mason [21], who noticed that the scale's iridescence emerged from below a mesh structure. This structure, the upper lamina, was later recognized to be a very elaborate formation of the crossribs, the scale elements that connect adjacent ridges [2,22,23]. Compared to the lower lamina, the upper lamina is relatively thick (~200 and 1000 nm, respectively), arguably because of the necessity of storing sufficient pigment so that an effective high pass filter can be realized [32], but otherwise this thick layer does not significantly alter the reflectance from the lower lamina, since introduced modulations are effectively averaged out. A peak absorbance of ~0.6 was measured in scales immersed in a refractive index matching fluid, but of course effectively twice this value holds for the light that is ultimately reflected from the lower lamina. The important outcome of this study is that the variation in the thicknesses of the multilayers causes a strongly smoothed reflectance spectrum. Generally in biological photonic systems small variations in the anatomical properties will occur already at the micrometer scale. Optical spectra are virtually always measured from areas with size well above the micrometer scale and therefore this will result in substantially smoothed spectra [33–35].

The blue-green fluorescence emission that is generated by the strongly absorbing pigment present in the investigated papilionids is certainly reflected by the DBR of the bottom lamina, but the contribution to the appearance offered by this fluorescence has been measured to be negligible (see ref [32].).

The structural organization of the cover scales of the papilionids *Parides sesostris* and *Teinopalpus imperialis* is similar to that of the cover scales of the *nireus* group papilionids [7,36–38]. In all cases, a thick elaborate upper lamina is situated above a reflecting photonic structure. In *P. sesostris* and *T. imperialis*, however, a so-called honeycomb structure is immediately on top of a layer composed of gyroid domains, which act as 3D photonic crystals [17,18,20]. Not unlike the *nireus* group of butterflies, the cover scales of *P. sesostris* have a distinct green color, but upon removal of the upper lamina a blue color remains [19,38]. These

#162309 - $15.00 USD Received 31 Jan 2012; revised 23 Mar 2012; accepted 23 Mar 2012; published 2 Apr 2012

scales therefore contain a blue-absorbing pigment in the upper lamina which also functions in this case as a long-pass filter for the underlying structurally colored region [19].

The studied papilionid species have revealed a novel technique to fine-tune the butterfly wing coloration to a narrowband blue-green, in addition to other methods that have been already discovered, for instance, with sculpted multilayers of *P. palinurus* and *P. blumei* scales [31,39], perforated multilayers in lycaenids [15], gyroid 3D-photonic crystals of the lycaenid *Callophrys rubi* and the papilionids *Papilio sesostris* [17–20], and bile pigments of *Graphium* species and other papilionids and nymphalids [40,41]. Interestingly, in the latter case certain species (e.g. *Graphium sarpedon*) use a long-pass filter (lutein) to change the pigmentary coloration due to the bile pigment sarpedobilin from blue into green [42], not dissimilar to the case of the four *nireus* papilionids and *P. sesostris* that use a long-pass filter to change the wing color; however, here the coloration has a structural basis. Butterflies can clearly employ a rich variety of optical tools to tune their colors.

Acknowledgments

We thank H.L. Leertouwer for assistance. Financial support was given by AFOSR grants FA8655-08-1-3012 and FA9550-10-1-0020 and the School of Physics at The University of Exeter.

#162309 - $15.00 USD Received 31 Jan 2012; revised 23 Mar 2012; accepted 23 Mar 2012; published 2 Apr 2012